



This information is current as of September 3, 2015.

Transcription Factor 7 Limits Regulatory T Cell Generation in the Thymus

Melanie M. Barra, David M. Richards, Jenny Hansson, Ann-Cathrin Hofer, Michael Delacher, Jan Hettinger, Jeroen Krijgsveld and Markus Feuerer

J Immunol published online 31 August 2015
<http://www.jimmunol.org/content/early/2015/08/30/jimmunol.1500821>

Supplementary Material <http://www.jimmunol.org/content/suppl/2015/08/30/jimmunol.1500821.DCSupplemental.html>

Subscriptions Information about subscribing to *The Journal of Immunology* is online at:
<http://jimmunol.org/subscriptions>

Permissions Submit copyright permission requests at:
<http://www.aai.org/ji/copyright.html>

Email Alerts Receive free email-alerts when new articles cite this article. Sign up at:
<http://jimmunol.org/cgi/alerts/etc>

Transcription Factor 7 Limits Regulatory T Cell Generation in the Thymus

Melanie M. Barra,* David M. Richards,* Jenny Hansson,[†] Ann-Cathrin Hofer,* Michael Delacher,* Jan Hettinger,* Jeroen Krijgsveld,[†] and Markus Feuerer*

Regulatory T cells (Tregs) differentiate in the thymus, but the mechanisms that control this process are not fully understood. We generated a comprehensive quantitative and differential proteome of murine Tregs and conventional T cells. We identified 5225 proteins, 164 of which were differentially expressed in Tregs. Together with the comparative analysis of proteome and gene expression data, we identified TCF7 as a promising candidate. Genetic elimination of transcription factor 7 (TCF7) led to increased fractions of Tregs in the thymus. Reduced levels of TCF7, found in the heterozygote, resulted in a greater potential for Treg precursors to differentiate into the Treg lineage. In contrast, activation of TCF7 through β -catenin had the opposite effect. TCF7 levels influenced the required TCR signaling strength of Treg precursors, and TCF7 deficiency broadened the repertoire and allowed lower TCR affinities to be recruited into the Treg lineage. FOXP3 was able to repress TCF7 protein expression. In summary, we propose a regulatory role for TCF7 in limiting access to the Treg lineage. *The Journal of Immunology*, 2015, 195: 000–000.

Regulatory T cells (Tregs) are indispensable in the regulation of immune responses throughout life. They ensure immune homeostasis and bring inflammation to a proper resolution. They are characterized by the expression of FOXP3, which was identified as the major transcription factor and is crucial for Treg function (1–3). Dysfunction or impaired development of Tregs leads to severe autoimmune diseases (4). The thymus has a dual role in T cell tolerance: by the negative selection of autoreactive T cells and by the generation of the thymus-derived Treg (tTreg) pool (5).

T cell maturation in the thymus is a multistep process that involves different molecular and cellular mechanisms. T cell precursors sequentially differentiate from the immature CD4 and CD8 double-negative (DN) stage to the CD4 and CD8 double-positive (DP) stage. Finally, they develop into CD4 or CD8 single-positive (SP) thymocytes (6). During this transition between positive and negative selection, some precursors get committed to the Treg

lineage in a process that still needs to be resolved in detail. Analysis of mice with limited TCR diversity demonstrated only little overlap in the TCR CDR3 sequences between Tregs and conventional CD4⁺ T cells (Tconvs), indicating that different TCR specificities could account for the alternative fate (7–9). TCR signaling strength seems to have an important role in the selection into the Treg lineage, and several studies suggested that Tregs have a higher level of self-reactivity than Tconvs (5). It is believed that Treg development in the thymus occurs in a window during which the TCR avidity for self-antigens lies close to or even overlaps with the avidity range, leading to negative selection (5). This is supported by *Nr4a1(Nur77)-GFP* reporter mice, in which the TCR signal strength, as measured by reporter activity, required for Treg differentiation is substantially higher than for Tconvs (10). In addition to TCR signaling, other factors contribute to the Treg lineage decision. Intraclonal competition, likely caused by limited access to Ag (11), and costimulation via CD28 are important variables (12). The two common γ -chain cytokines IL-2 and IL-15 are additional factors that are essential for Treg differentiation (13, 14). In fact, it was proposed that Treg development occurs in two consecutive steps. The first step is TCR dependent, whereas the second step is TCR independent but requires common γ -chain signaling by IL-2 or IL-15 (13). Each of these steps has corresponding precursor populations in the thymus: the “early Treg precursor” is defined as CD4SP CD69⁺CD25[−]FOXP3[−], and the “late Treg precursor” is characterized as CD4SP CD69⁺CD25⁺FOXP3[−] (13, 14).

Transcription factor 7 (TCF7; also known as TCF1) is important for T cell development in the thymus. *Tcf7*-deficient (*Tcf7*^{−/−}) mice have greatly reduced numbers of thymocytes (15), and it was shown that TCF7 is involved in thymocyte differentiation at several important checkpoints (16–18). The early T cell precursors require TCF7 for efficient T cell lineage specification and differentiation (19, 20). TCR β selection and the maturation of DN thymocytes to the DP stage are compromised (15, 17). In DN and preselected DP thymocytes, TCF7 restrains expression of lymphoid enhancer-binding factor 1 (LEF1) and components of the Notch signaling pathway to prevent malignancy (21). TCF7 was also shown to promote commitment into the CD4⁺ T cell lineage (22). Lastly, negative selection and cell survival at the DP stage also were shown to depend on TCF7 (23, 24). Because this is the

*Immune Tolerance, Tumor Immunology Program, German Cancer Research Center, 69120 Heidelberg, Germany; and [†]Genome Biology Unit, European Molecular Biology Laboratory, 69117 Heidelberg, Germany

Received for publication April 8, 2015. Accepted for publication July 23, 2015.

This work was supported by grants from the Helmholtz Association of German Research Centers (HZ-NG-505 to M.F.) and the Netherlands Organization for Scientific Research (to J.K.). M.M.B. and J. Hettinger were supported by Helmholtz Association of German Research Centers Ph.D. fellowships; A.-C.H. was supported by the Cooperation Program in Cancer Research of the German Cancer Research Center and Israel’s Ministry of Science, Technology and Space; and M.D. was supported by the German-Israeli Helmholtz Research School in Cancer Biology.

The mass spectrometry proteomics data presented in this article have been submitted to the ProteomeXchange Consortium (<http://www.proteomexchange.org>) under accession number PXD000794.

Address correspondence and reprint requests to Dr. Markus Feuerer, Immune Tolerance, Tumor Immunology Program, German Cancer Research Center, Im Neuenheimer Feld 280, 69120 Heidelberg, Germany. E-mail address: m.feuerer@dkfz-heidelberg.de

The online version of this article contains supplemental material.

Abbreviations used in this article: B6, C57BL/6; BIO, 6-bromoindirubin-3'-oxime; BM, bone marrow; CHIR99021, 6-[(2-[4-(2,4-Dichlorophenyl)-5-(5-methyl-1H-imidazol-2-yl)-2-pyrimidinyl]amino)ethyl]amino]-3-pyridinecarbonitrile; DN, double negative; DP, double positive; K14, keratin 14; LEF1, lymphoid enhancer-binding factor 1; LN, lymph node; MS, mass spectrometry; SP, single positive; TCF7, transcription factor 7; Tconv, conventional CD4⁺ T cell; Treg, regulatory T cell; tTreg, thymus-derived Treg.

Copyright © 2015 by The American Association of Immunologists, Inc. 0022-1767/15/\$25.00

stage when TCR-mediated positive and negative selection of thymocytes occurs, an obvious question is whether TCF7 also influences Treg generation in the thymus.

Gene expression profiles of Tregs from different tissues and subphenotypes, as well as under various activation conditions, have been studied (25–28). Those studies revealed important information about Treg molecular signatures on the mRNA level; however, a precise description of the Treg proteome and its correlation with mRNA expression are lacking.

In this study, we analyzed the whole proteome of Tregs compared with Tconvs and identified TCF7 as an interesting candidate. Based on its known function during thymocyte development, we investigated the role of TCF7 in tTreg differentiation and demonstrated that its presence restricts the development of tTregs. TCF7 deficiency broadened the repertoire and allowed lower TCR affinities to be recruited into the Treg lineage.

Materials and Methods

Mice

Wild-type C57BL/6 (B6) mice were obtained from the Charles River Breeding Laboratories (Wilmington, MA) or The Jackson Laboratory (Bar Harbor, ME). *Tcf7*^{-/-} mice (*Tcf7*^{tm1Cle}, ΔVII) were a gift from Hans Clevers (Hubrecht Institute, Utrecht, The Netherlands) (15). *Tcf7*^{-/-} mice were crossed to *Foxp3*-YFP mice [B6.129(Cg)-*Foxp3*^{tm4(YFP/cre)Ay}J; Jackson catalog no. 016959] (29) or *Nr4a1*-GFP mice [Tg(Nr4a1-EGFP/cre)820Khog/J; Jackson catalog no. 016617] (10) in the German Cancer Research Center animal facility. We used littermates as control animals for all experiments. *Foxp3*-GFP mice [B6.129(Cg)-*Foxp3*^{tm3(DTR/GFP)Ay}J; Jackson catalog no. 016958] (30) were crossed to a CD45.1 (B6.SJL-Ptprc^aPepc^b/BoyJ; Jackson catalog no. 002014) or CD90.1 (B6.PL-Thy1^a/CyJ; Jackson catalog no. 000406) background. All mice were maintained under specific pathogen-free conditions in the animal facility of the German Cancer Research Center. All animal experiments were reviewed and approved by the governmental committee for animal experimentation in Karlsruhe, Germany.

Tissue isolation and sample preparation

For tissue isolation, spleen, thymus, and lymph nodes (LN; axillary, brachial, and inguinal) were removed, and organs were processed by mashing and filtering to prepare single-cell suspensions. Ammonium chloride–potassium bicarbonate lysis buffer was used to lyse erythrocytes in spleen samples. Samples that were purified by FACS for Treg protein isolation (mass spectrometry [MS] experiments) were first enriched for CD25. Samples that were purified by FACS for Treg precursors and quantitative real-time PCR experiments were first depleted of CD8⁺ cells. For enrichment and depletion, cells were labeled with biotin-conjugated Abs and anti-biotin MicroBeads (Miltenyi Biotec). Magnetic cell separation was performed using an AutoMACS Pro Separator (Miltenyi Biotec).

Flow cytometry

Cells were labeled with Abs/streptavidin: CD3ε (145-2C11), CD4 (RM4-5 or GK1.5), CD5 (53-7.3), CD8α (53-6.7), CD11b (M1/70), CD11c (N418), CD19 (6D5), CD25 (PC61), CD44 (IM7), CD61 (2C9.G2 [HMB3-1]), CD69 (H1.2F3), CD86 (GL-1), CD122 (5H4), CD304 (N43-7), CD357 (DTA-1), Foxp3 (FJK-16s) (all from BD Pharmingen, BioLegend or eBioscience); LEF1 (C12A5) and TCF1 (C63D9) (from Cell Signaling); and keratin 14 (K14; polyclonal; Covance). Immunohistochemical staining of cells was performed using the IC Foxp3 Staining Buffer Set (eBioscience). Cells were kept on ice at all times unless they were fixed. Cells were analyzed using the BD Bioscience Canto II or LSR II. FACSAria I, II, and III instruments (BD Biosciences) were used for FACS purification of cells. Purity of cell sorts was assured through postsort analysis. FlowJo (TreeStar) was used to analyze flow cytometry data.

Cell counting

For counting of total thymus subpopulations using beads, AccuCheck Counting beads (Invitrogen) were added to the sample prior to acquisition. A total of 2×10^4 beads was added to 20% of the thymus sample. The number of cells in the total thymus was calculated according to the manufacturer's instructions.

For *in vitro* experiment cell counts, an identical number of cells was seeded in all wells. All cells were stained and completely acquired by flow cytometry.

In vitro Treg-differentiation assay

FACS-purified early (CD4SP CD69⁺CD25⁻FOXP3⁻) or late (CD4SP CD69⁺CD25⁺FOXP3⁻) Treg precursors were seeded at 1×10^5 cells/well in 96-well round-bottom plates and cultured for 1 or 3 d before analysis. Cells were cultured with different combinations of human IL-2 (100 U/ml; Proleukin S; Novartis), murine IL-15 (100 ng/ml; PeproTech), and anti-CD3/CD28 Dynabeads (Invitrogen) at a cell/bead ratio of 1:1.

For Wnt-activation assays, 1×10^5 sorted Treg precursors were cultured under the conditions described above. In addition, DMSO-dissolved Wnt-activator 6-bromoindirubin-3'-oxime (BIO) or 6-[2-[[4-(2,4-Dichlorophenyl)-5-(5-methyl-1H-imidazol-2-yl)-2-pyrimidinyl]amino]ethyl]amino]-3-pyridinecarbonitrile (CHIR99021) (both from BIOMOL) was added to the cultures at 1 or 2 μM. Control wells were cultured with DMSO concentrations corresponding to the highest DMSO content in the wells containing the Wnt activators.

For the *in vitro* Treg-differentiation assay with titration of anti-CD3 stimulus, 96-well flat-bottom plates were coated overnight with different concentrations (0.1, 0.25, 0.5, or 2 μg/ml) of purified anti-CD3 in PBS. Plates were washed with PBS prior to use. Purified anti-CD28 (10 μg/ml) was added together with 1×10^5 Treg precursors, IL-2, and IL-15 to the culture media.

For flow cytometric analysis of all *in vitro* experiments, Fixable Viability Dye eFluor 506 (eBioscience) was used to exclude dead cells.

Immunofluorescence imaging

Sections (5 μm) from cryopreserved thymi from *Tcf7*^{+/+} and *Tcf7*^{-/-} mice were prepared by step sectioning every 25 μm. Samples were fixed in ice-cold acetone, blocked in PBST with 5% (v/v) FCS and 1% (w/v) BSA, and stained with Ab against K14 (Covance). Next, sections were stained with Anti-Rabbit IgG–Alexa Fluor 488 (Jackson ImmunoResearch) and DAPI (Sigma). Imaging was performed on an AxioImager.Z1 microscope (Zeiss). Images were analyzed in AxioVision (Zeiss) and Photoshop (Adobe).

Quantitative real-time PCR

Cells were FACS purified into TRIzol reagent (Life Technologies), and mRNA was extracted according to the manufacturer's protocol. For cDNA synthesis, SuperScript reverse transcriptase (Invitrogen) and oligo(dT) primers were used. cDNA samples were analyzed by quantitative real-time PCR using Power SYBR Green Master Mix and the ViiA 7 system (both from Life Technologies). Appropriate primers for *Hprt* and *Tcf7* were used. The following primer sequences were used: *Hprt* ForP: 5'-CTT-TGCTGACCTGCTGGATT-3' and *Hprt* RevP: 5'-TATGTCCCCCGTT-GACTGAT-3' and *Tcf7* ForP: 5'-CGAGAACAGCAGGCCAAGTA-3' and *Tcf7* RevP: 5'-CCTGTGGTGGATTCTTGATG-3'. *Tcf7* mRNA (gene X) abundance was quantified as percentage relative to the expression of *Hprt* by the change-in-threshold method (100*(relative expression = $2^{(CT(\text{gene X}) - CT(Hprt))}$)).

Retroviral transduction of FOXP3

Phoenix-ECO cells were transfected with calcium phosphate using a murine stem cell virus plasmid (IRES-CD90.1, empty or encoding wild-type human FOXP3) (28). Supernatants containing murine stem cell virus retroviral particles were harvested at day 3 after transfection. Wells were prepared for T cell culture by coating with goat-anti-hamster IgG (MP Biomedicals), followed by purified anti-CD3 and anti-CD28. LN and spleen cells were depleted of CD8, CD19, CD11b, CD11c, CD25, and CD49b using an AutoMACS Pro Separator (Miltenyi Biotec) to enrich for Tconvs. T cells were seeded at 2.5×10^6 per well in a precoated 24-well plate. IL-2 (20 U/ml) was added to the T cell culture. T cells were spin-transduced with fresh viral supernatants containing Polybrene (Sigma-Aldrich) ~40 h after the start of T cell stimulation. Retrovirally transduced T cells were identified by CD90.1 expression and analyzed 3 d after transduction.

Protein digestion, labeling of peptides with stable isotopes, and fractionation

FACS-purified cell pellets were snap-frozen in liquid nitrogen. After lysis of cells in 0.1% RapiGest (Waters)/50 mM ammonium bicarbonate, extracted proteins were reduced/alkylated with 5 mM DTT and 10 mM iodoacetamide and digested overnight with sequencing-grade modified trypsin (Promega). Resulting peptides were dimethyl labeled on a column, as previously described (31). Briefly, peptides were labeled on Sep-Pak C₁₈ cartridges (Waters) with the labeling reagent ("light" or "intermediate") using CH₂O [Fisher] + NaBH₃CN [Fluka] or CD₂O [Isotec] + NaBH₃CN, respectively). In the second, third, and fourth biological replicate experiments, cell population reagents were swapped. The "light"- and "intermediate"-labeled samples were mixed at a 1:1 ratio based on cell number. Sample complexity

was reduced by fractionating the peptides with pH 3–10 IPG strips and a 3100 OFFGEL Fractionator (Agilent) into 12 fractions.

Liquid chromatography–electrospray ionization–tandem MS analysis

Peptides were separated using the nanoACQUITY UPLC system (Waters) fitted with a trapping column (nanoACQUITY Symmetry C18, 5 μ m particle size, 180 μ m inner diameter \times 20 mm length) and an analytical column (nanoACQUITY BEH C18, 1.7 μ m particle size, 75 μ m inner diameter \times 200 mm length). Peptides were separated on a 120-min gradient and analyzed by electrospray ionization–tandem MS on an LTQ Orbitrap Velos (Thermo Fisher Scientific). Full-scan spectra from m/z 300 to 1700 at resolution 30,000 FWHM (profile mode) were acquired in the Orbitrap MS. From each full-scan spectra, the 15 ions with the highest relative intensity were selected for fragmentation in the ion trap. A lock mass correction using a background ion (m/z 445.12003) was applied.

Protein identification and quantification

MS raw data files were processed with MaxQuant (version 1.2.0.18) (32). Cysteine carbamidomethylation and methionine oxidation were selected as fixed and variable modifications, respectively. The derived peak list was searched using the built-in Andromeda search engine (version 1.2.0.18) in MaxQuant against the Uniprot mouse database (2011.06.21). Initial maximal allowed mass tolerance was set to 20 ppm for peptide masses, followed by 6 ppm in the main search, and 0.5 Da for fragment ion masses. A 1% false discovery rate was required at the protein level and the peptide level. In addition to the false discovery rate threshold, proteins were considered identified if they had at least one unique peptide. The protein identification was reported as an indistinguishable “protein group” if no unique peptide sequence to a single database entry was identified.

Bioinformatic and statistical analysis

Statistical analysis was performed for the proteins quantified in at least two replicates using the Limma package in R/Bioconductor (33, 34). Proteins with an adjusted *p* value < 0.05 were considered differentially expressed between Tregs and Tconvs. Network analysis was done using STRING (35), and visualization was performed in Cytoscape v2.8 (36).

Treg-specific genes (over- and underrepresented) were identified based on RNA microarray expression data that we published earlier (25, 28). Tregs and Tconvs from LN and thymus were included. Genes that were differentially expressed >1.5 -fold between Tregs and Tconvs were considered significantly different (*p* < 0.05 , Student *t* test, two-tailed). Generated gene lists were cross-referenced with our proteomic data based on gene names and used for further analysis.

Statistical analysis of experimental data was performed using Prism software (GraphPad) or Excel (Microsoft). The statistical tests and corresponding parameters used are included in the figure legends. Results were considered statistically significant at *p* < 0.05 .

Accession numbers

The MS proteomics data have been submitted to the ProteomeXchange consortium (<http://www.proteomexchange.org>) via the PRIDE partner repository (37) under dataset identifier PXD000794.

Results

Differential quantitative MS of the Treg proteome

We performed MS-based quantitative proteomic analysis of murine Tregs, comparing them with Tconvs. To this end, cells were highly enriched by FACS, and proteins were isolated and differentially labeled with stable isotopes (31) (Fig. 1A). Peptide fractions were analyzed by high-resolution nano liquid chromatography–tandem MS, and relative protein abundance was based on relative MS signal intensities (Fig. 1B). Four replicates identified a total of 5225 unique proteins, with 4859 detected in at least two replicates and 3756 detected in all replicates (Fig. 1C, Supplemental Table I). The identified proteins covered all protein classes and cell compartments, from the nucleus to the cell surface (Fig. 1D). Among the identified proteins, 164 were significantly (*p* < 0.05) differentially expressed between Tregs and Tconvs (Supplemental Table I). Of these, 51 proteins were underrepresented and 113 proteins were overrepresented in Tregs. The quantified proteins are plotted as fold change Treg versus Tconv against *p* value to visualize differences (Fig. 2A).

Classic Treg markers, such as FOXP3, GARP, IL-2R β , GITR, and NRP1, were highly overrepresented in Tregs compared with Tconvs. To confirm the MS data, we stained Tregs and Tconvs with available Abs and performed flow cytometry (Fig. 2B, 2C). Fold changes between Tregs and Tconvs, detected by MS and flow cytometry, showed a high correlation ($R^2 = +0.8017$, *p* < 0.0001) (Fig. 2D).

To get an insight into the correlation between mRNA and protein expression and possible posttranscriptional regulation, we mapped our proteome data onto our previously published mRNA gene expression data (25, 28). Comparison of the significantly over- and underrepresented proteins with gene expression data showed an overall strong correlation (*p* < 0.0001) (Fig. 3A, left panels). Similarly, significantly over- and underrepresented genes correlated with protein data (*p* < 0.0001) (Fig. 3A, right panels), indicating that, in most cases, protein expression follows mRNA expression.

Fold change to fold change comparisons of significantly differentially expressed proteins and mRNA showed a reasonably good correlation for most of the candidates (Fig. 3B). However, this also revealed interesting targets with strong differential expression exclusively at the mRNA or protein level (e.g., SLC4A1 and DNM2), possibly pointing to the involvement of more intricate posttranscriptional regulatory mechanisms.

We then subdivided the 164 differentially expressed proteins by function and location. Proteins associated with the plasma membrane, kinases or transcription factors, included already known, but also unappreciated, candidates (Fig. 3C).

Expression of the transcription factor TCF7 in Tregs

For the accurate function and differentiation of cells, it is often essential to repress the expression of specific genes. Therefore, we were particularly interested in underrepresented proteins in Tregs. To screen for interesting targets, we compared LN and thymus mRNA expression data sets (25, 28) with the set of 51 proteins underrepresented in Tregs. We were able to map 43 protein candidates to gene expression data and, thereby, identified a cluster of genes that was prominently underrepresented in Tregs (Fig. 4A, highlighted in red). This cluster included three genes that were previously described in the context of Treg development and function (Fig. 4A): *Pde3b*, *Satb1*, and *Itk* (38–40). This cluster also contained *Tcf7*, which was one of the most strongly underrepresented proteins in Tregs (Supplemental Table I). *TCF7* was established to be important during thymocyte differentiation (15), but its function in the context of tTreg generation has not been analyzed.

Recently, a *Tcf7-Lef1* coregulated cluster of genes was described by the Immunological Genome Consortium (41). We compared this *Tcf7-Lef1* coregulated cluster with our proteomics data and identified 19 members in our data set (Fig. 4B). Those included, in addition to *TCF7* and *LEF1*, THEMIS, ITK, and multiple CD3 family members. Interestingly, the whole cluster was significantly (*p* = 0.00015) underrepresented in Tregs in our proteome data set (Fig. 4B, 4C).

The data obtained from our quantitative MS analysis identified *TCF7* as significantly underrepresented in Tregs, and it was differentially expressed on the gene level. Hence, we performed intracellular flow cytometric staining for *TCF7* and *LEF1* and confirmed that both were underrepresented in Tregs, as detected by our MS analysis (Fig. 4D, 4E). Because our comparative proteomics data set identified the transcription factor *TCF7* as a promising target differentially expressed in thymic Tregs, we wondered about its role in tTreg generation.

Dosage effect: reduction in *TCF7* results in greater Treg-generation capacity

To study the role of *TCF7* in thymic Treg differentiation, we analyzed a *Tcf7*-deficient mouse model (15). Flow cytometric analysis

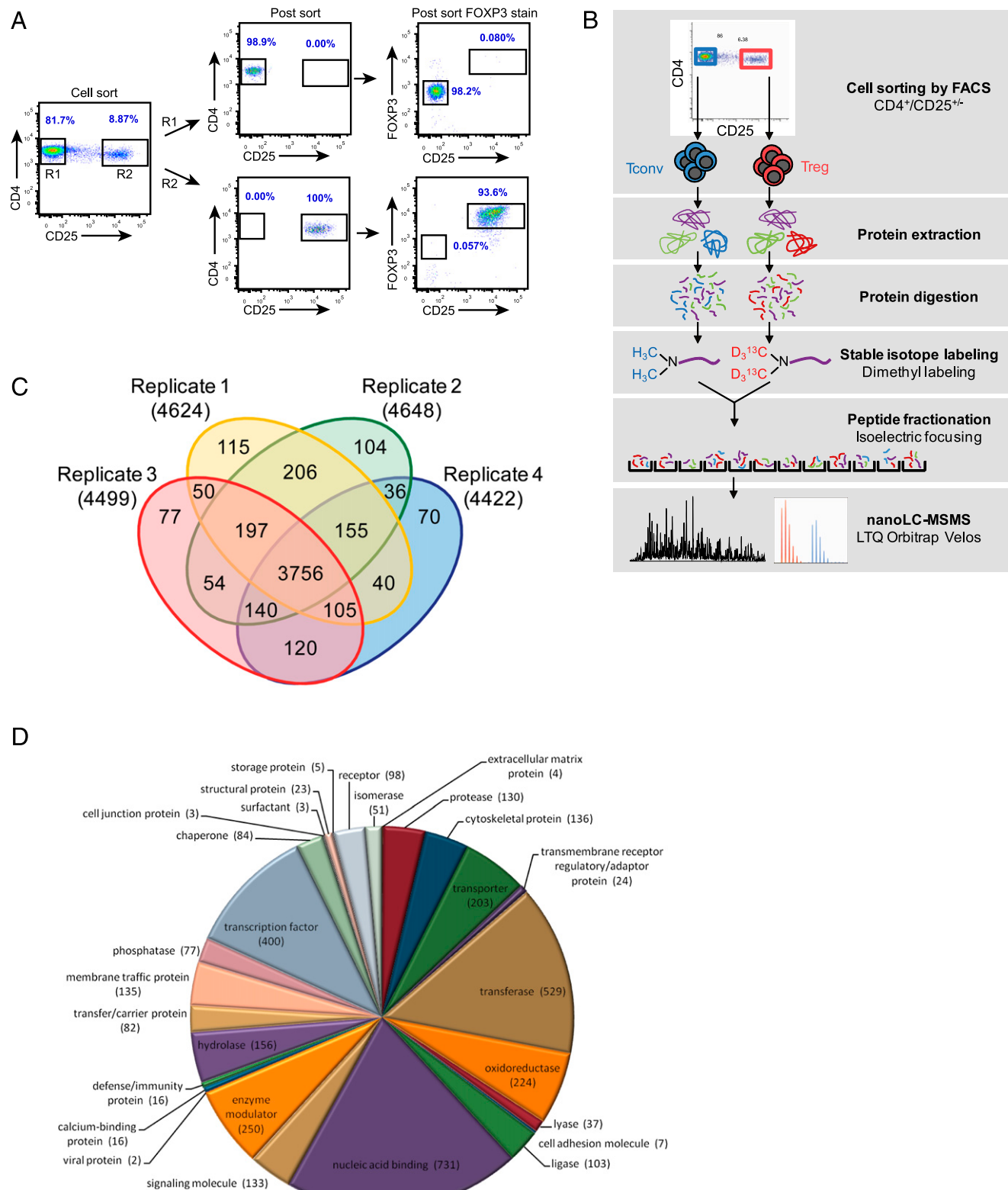


FIGURE 1. Differential quantitative MS workflow. **(A)** Sort gates for Tregs (R2; CD4⁺CD25^{high}) and Tconvs (R1; CD4⁺CD25⁻). Postsort control of R1 and R2 cell populations and postsort intracellular FOXP3 staining. Numbers show percentages of cells within the indicated box. **(B)** Proteomics work flow. **(C)** Venn diagram of the quantified proteins in four replicates. **(D)** Pie chart of protein classes among the identified proteins.

and cell counting showed that the total numbers of DN, DP, CD4 and CD8 SP thymocytes were reduced in *Tcf7*^{-/-} mice compared with the heterozygous (*Tcf7*^{+/−}) and wild-type (*Tcf7*^{+/+}) littermate controls (Supplemental Fig. 1A). Immunohistological staining of

Tcf7^{-/-} and *Tcf7*^{+/+} thymi with K14, a marker for thymic medullary epithelial cells, showed an overall reduced thymus size but relatively normal organization into medullary and cortical regions (Supplemental Fig. 1B, 1C).

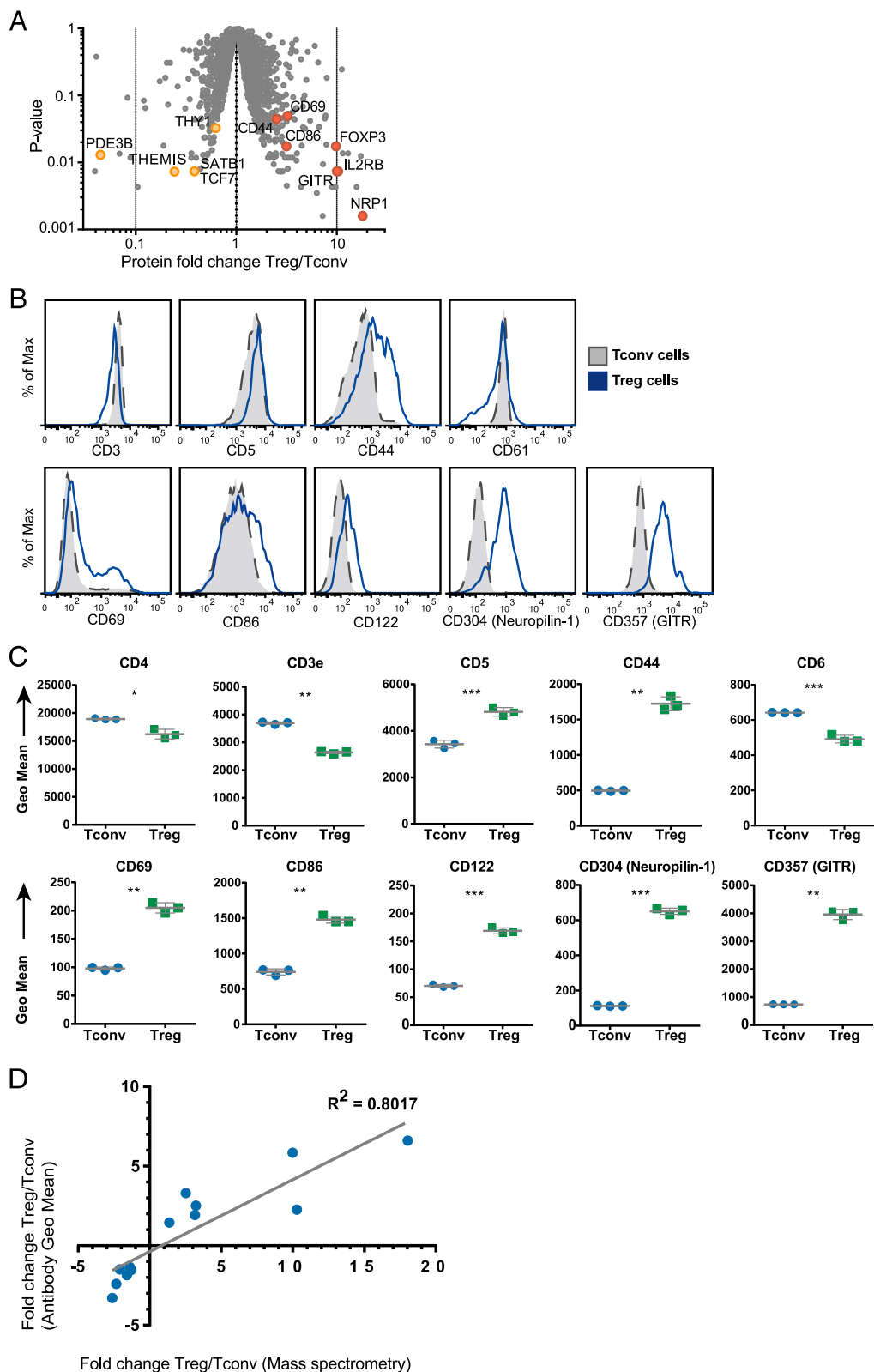


FIGURE 2. Confirmation of differential quantitative MS. **(A)** The 4859 proteins identified in at least two of four replicates are plotted as average Treg/Tconv fold change versus *p* value. Selected significantly over- or underrepresented proteins are depicted in red or orange, respectively. **(B)** Flow cytometric analysis of surface molecule expression on LN Tregs and Tconv identified as differentially regulated by MS. **(C)** Quantification of plots shown in **(A)** (*n* = 3). Data points represent individual animals. Data are mean + SD. **(D)** Correlation of Treg/Tconv protein fold changes detected by MS and flow cytometry. **p* < 0.05, ***p* < 0.01, ****p* < 0.001, unpaired *t* test.

When we analyzed the fraction of Tregs among the CD4 SP population, we found that *Tcf7*^{-/-} mice harbored approximately three times more thymic Tregs compared with *Tcf7*^{+/+} mice (5

versus 15%) (Fig. 5A). However, the total number of Tregs was not elevated, because there is also a reduction in the total number of CD4 SP cells in the *Tcf7*^{-/-} thymus (Supplemental Fig. 1A).

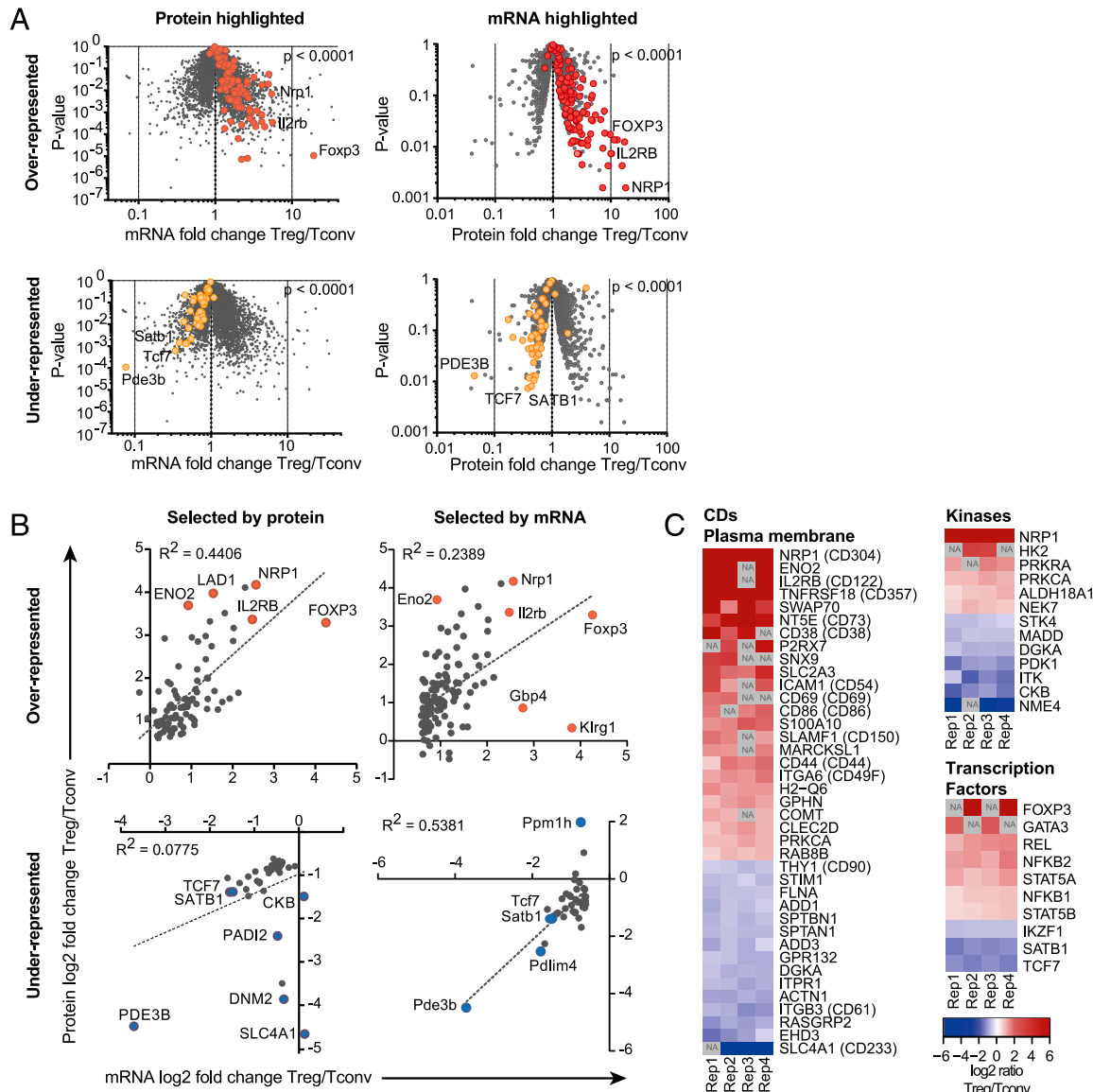


FIGURE 3. Proteomic analysis of Tregs and Tconv cells by differential quantitative MS. **(A and B)** Correlation of gene expression (mRNA) and proteomics data. (A) Significantly differentially expressed proteins are highlighted on the gene expression data set (*left panels*). Significantly differentially expressed genes are highlighted on the proteomic data set (*right panels*). Over- or under-represented targets are depicted in red or orange, respectively. The *p* values were calculated using the χ^2 test. (B) Comparison of mRNA and protein fold changes. Selected by significantly changed protein (*left panels*) and significantly changed mRNA (*right panels*). Selected over- or underrepresented targets are depicted in red or blue, respectively. **(C)** Protein expression heat map of groups: CD-listed and plasma membrane, kinases, and transcription factors of significantly differentially expressed proteins identified in two or more replicates. NA, not available in specific replicate.

Because FOXP3⁺ cells are detectable as early as the DP stage (42), we looked at DP cells and found that *Tcf7* deficiency resulted in a significantly increased fraction of FOXP3⁺ cells (Fig. 5B). These observations indicate that the presence of TCF7 influences the frequency of Tregs in the thymus.

Because of the greatly reduced thymocyte number in *Tcf7*^{-/-} mice, it was not clear whether this increased Treg frequency in *Tcf7*^{-/-} mice was caused by influencing Treg development or by the decreased number of cells in the Tconv compartment. Therefore, we investigated Treg differentiation in heterozygous *Tcf7*^{+/−} mice, which had normal thymocyte numbers. Examination of TCF7 expression levels in thymus, LN, and spleen cells from *Tcf7*^{+/+}, *Tcf7*^{+/−}, and *Tcf7*^{-/-} mice showed a significant decrease in TCF7 expression in Tregs and Tconv in *Tcf7*^{-/-} mice compared with the *Tcf7*^{+/+} littermate mice (Fig. 5C, Supplemental Fig. 2A). In contrast, no difference was observed for the expression

level of LEF1 in the thymus, LN, and spleen between *Tcf7*^{+/+} and *Tcf7*^{-/-} mice (Supplemental Fig. 2B).

These results showed that *Tcf7*^{+/−} mice are an ideal model to study the dosage effect of *Tcf7* expression in the absence of significant changes in total thymocyte numbers. Because we were interested in tTreg differentiation, we analyzed Treg precursors, including the TCR-dependent early Treg precursor (CD4SP CD69⁺CD25[−]FOXP3[−]), as well as the TCR-independent, but common γ-chain signaling-dependent, late Treg precursor (CD4SP CD69⁺CD25⁺FOXP3[−]) (13, 14). *Tcf7*-specific real-time PCR revealed that gene expression levels of *Tcf7* in both Treg precursor populations in *Tcf7*^{+/−} mice were about half those in *Tcf7*^{+/+} mice (Fig. 5D).

Next, we analyzed the thymic Tregs and Treg precursors more closely in *Tcf7*^{+/−} mice. In line with the previous observation in *Tcf7*^{-/-} mice, the percentages of CD4SP FOXP3⁺ Tregs and late

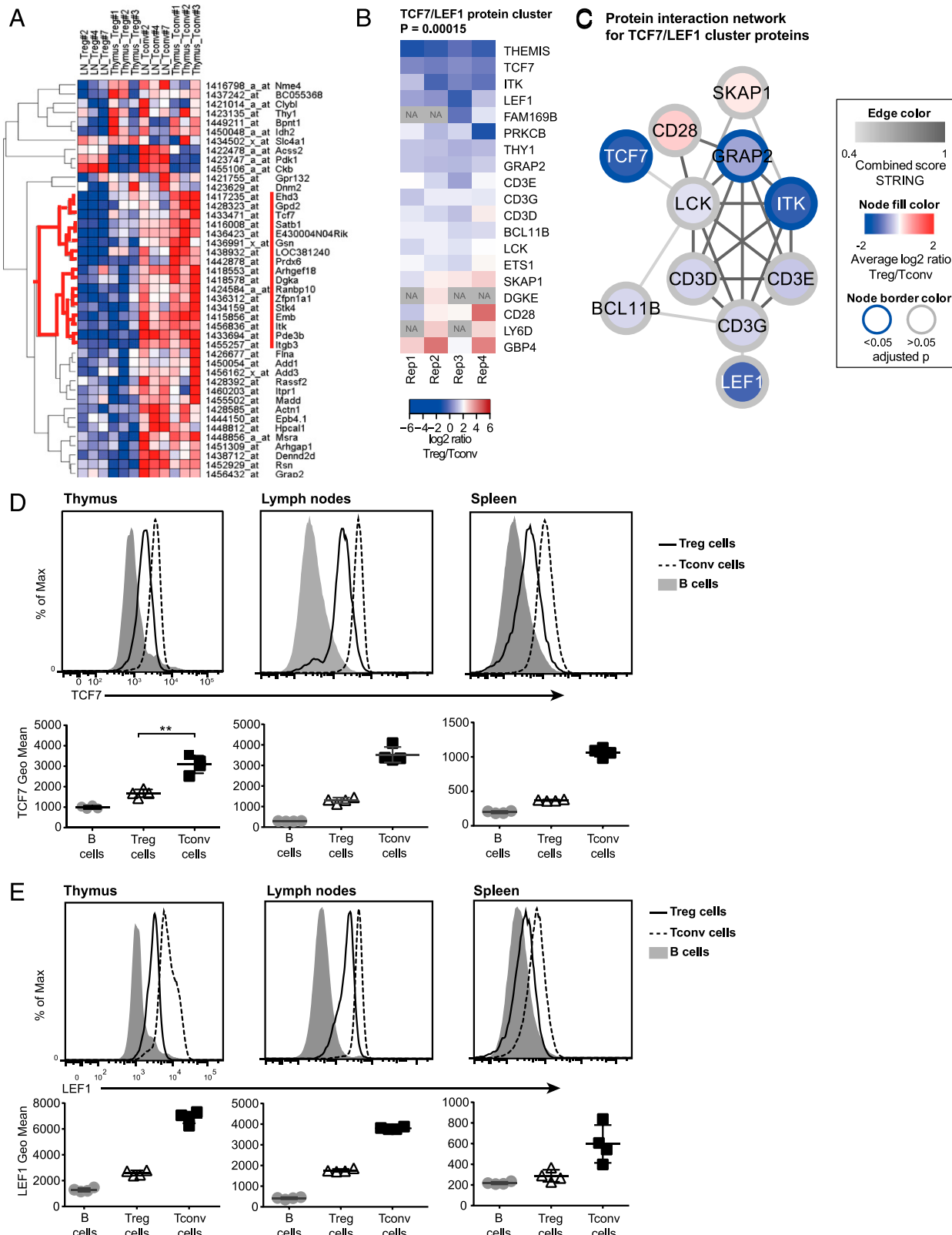


FIGURE 4. Identification of TCF7 and confirmation of TCF7 and LEF1 expression. **(A)** Heat map of gene expression of Tregs and Tconvs isolated from LN or thymus with the greatest (red) and least (blue) gene expression. Genes were selected from the 43 significantly underrepresented proteins (Tregs compared with Tconvs) identified by differential MS. Hierarchical clustering using Pearson's correlation (row normalized). Red line marks cluster. **(B)** Heat map of the TCF7/LEF1-coregulated cluster-related proteins. **(C)** Force-directed STRING network of interacting proteins from the TCF7/LEF1 cluster. Flow cytometric analysis of intracellular TCF7 **(D)** and LEF1 **(E)** expression in Tregs, Tconvs, and B cells from thymus, LN, and spleen of *Tcf7^{+/+}* mice ($n = 4$). B cells served as a negative control. Symbols represent individual samples, and the horizontal lines indicate the mean value for each group. ** $p < 0.01$, unpaired t test.

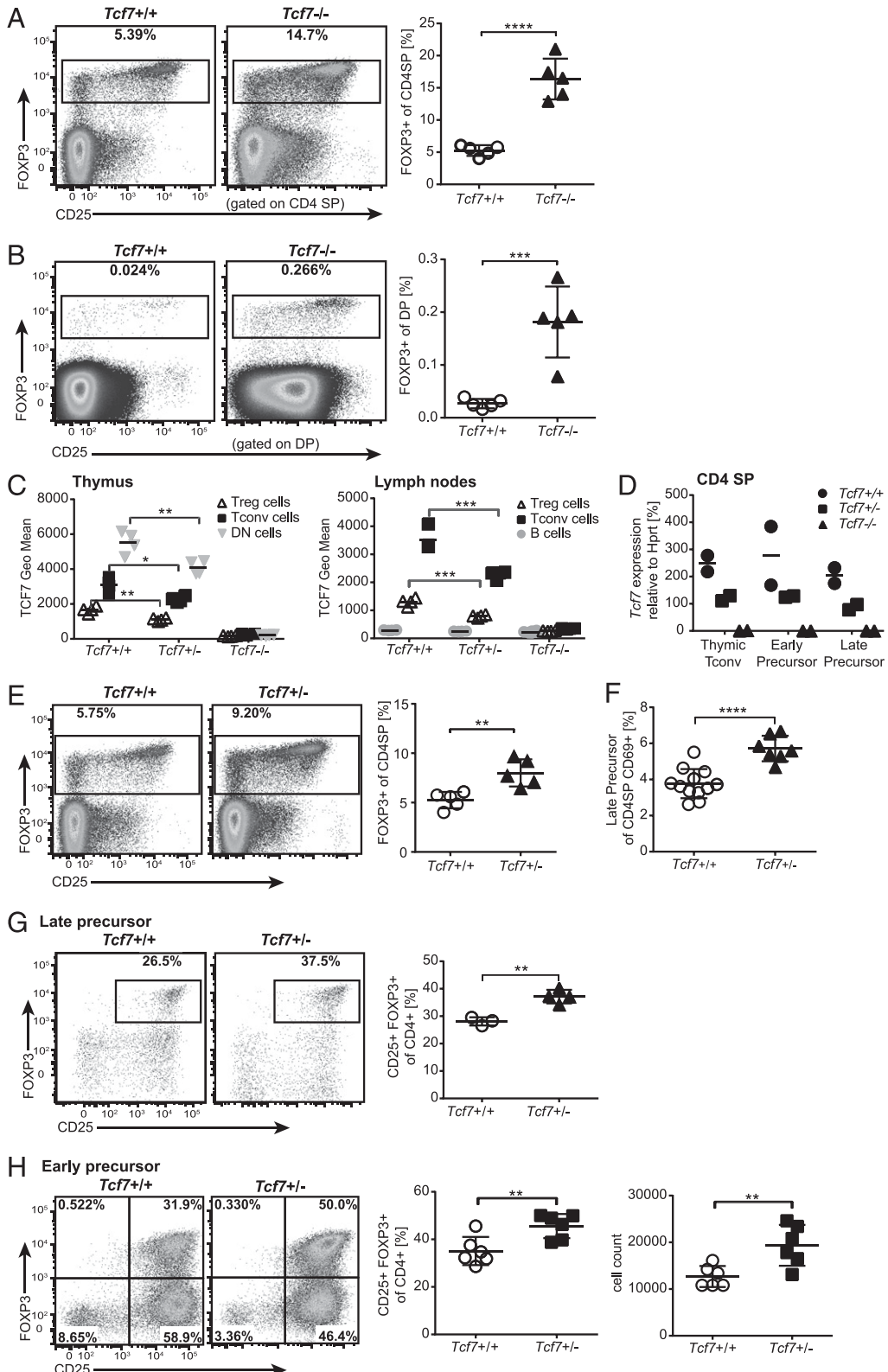


FIGURE 5. Reduction of TCF7 results in higher Treg-generation capacity. FOXP3 and CD25 expression in CD4SP cells ($n = 5$) (A) and DP cells ($n = 5$) (B) from *Tcf7^{+/+}* and *Tcf7^{-/-}* mice. (C) TCF7 expression in Tregs, Tconvs, B cells, and DN cells from thymus and LN from *Tcf7^{+/+}*, *Tcf7^{+/-}*, and *Tcf7^{-/-}* mice ($n = 4$). *Tcf7^{+/+}* data are also plotted in Fig. 4D. (D) *Tcf7* mRNA expression in FACS-purified thymic Tconvs and Treg precursors from *Tcf7^{+/+}*, *Tcf7^{+/-}*, and *Tcf7^{-/-}* mice via quantitative PCR. Data are presented as percentage relative to *Hprt* expression. (E) FOXP3 and CD25 expression in CD4SP cells from *Tcf7^{+/+}* and *Tcf7^{+/-}* mice ($n = 5$). (F) Late Treg precursor frequency in *Tcf7^{+/+}* and *Tcf7^{+/-}* mice ($n = 7-12$). Representative plots are shown in Supplemental Fig. 2C. (G and H) FOXP3 and CD25 expression in Treg precursors that were FACS purified from *Foxp3-YFP⁺* *Tcf7^{+/+}* and *Tcf7^{-/-}* mice and cultured in vitro. (G) The late Treg precursor was cultured for 1 d with IL-2 and IL-15 ($n = 3-4$). (H) The early Treg precursor was cultured for 3 d with IL-2 and anti-CD3/CD28 beads ($n = 6$). Cell count was determined by flow cytometry. Representative plots and quantification shown as described. Symbols represent individual samples, and numbers indicate the percentage of cells within the defined region. The horizontal lines indicate the mean value for each group. * $p < 0.05$, ** $p < 0.01$, *** $p < 0.001$, **** $p < 0.0001$, unpaired t test.

Treg precursors were significantly increased in *Tcf7^{+/−}* mice compared with *Tcf7⁺⁺* mice (Fig. 5E, 5F, Supplemental Fig. 2C). To confirm whether the identified precursor was the TCR signaling-independent late Treg precursor, we examined it in vitro. FACS-purified Foxp3[−] precursors (see gating scheme, Supplemental Fig. 2D, R4) were incubated with the cytokines IL-2 and IL-15 without TCR stimulus, and the expression of FOXP3 and CD25 was measured after 1 d in culture. *Tcf7^{+/−}* and *Tcf7⁺⁺* precursors differentiated into Foxp3-expressing Tregs, revealing that they were Treg-committed late precursors (Fig. 5G).

Initially, we tried to establish bone marrow (BM) chimera assays to analyze Treg differentiation. Unfortunately, because the development of TCF7-deficient progenitors into T cells is reduced, wild-type BM strongly outcompeted TCF7-deficient BM at all ratios tested [as previously described (19)]. Therefore, we decided to study purified precursors.

To study the early Treg precursor, a TCR-dependent and APC-free differentiation assay was established to avoid any influence from APCs (Supplemental Fig. 2E). The combination of IL-2, IL-15, and anti-CD3/CD28 bead-based stimulus generated the highest output of Tregs in terms of total number and frequency after 3 d of in vitro culture. Sixty to eighty percent of the cells differentiated into Tregs under these conditions (Supplemental Fig. 2E). As a control, we analyzed thymic Tconvs (CD4SP Foxp3[−]) that no longer expressed CD69 (CD69[−]); they had generally lost the ability to differentiate into Tregs under the same conditions, although they were strongly activated, induced CD25 expression, and proliferated (Supplemental Fig. 2E). Side-by-side comparison of FACS-purified early Treg precursors from *Tcf7^{+/−}* and *Tcf7⁺⁺* mice incubated with either the full stimulus (IL-2, IL-15, and anti-CD3/CD28 beads) or a weaker stimulus (without IL-15) showed that significantly more Tregs were generated from the *Tcf7^{+/−}* Treg precursor (Fig. 5H, Supplemental Fig. 2F).

The results obtained from the ex vivo analysis and in vitro culture suggest that decreased expression of TCF7 leads to enhanced Treg differentiation capacity.

TCF7 deficiency allows lower TCR affinities to be recruited into the Treg lineage

TCR signaling strength is a key factor that determines tTreg selection. The current model suggests that the TCR avidity that drives commitment into the Treg lineage is rather high and even overlaps with the affinity range of negative selection. CD5 expression was described to correlate with the overall avidity of the MHC–TCR interaction during positive selection (43). Tregs show higher levels of CD5 on the surface compared with Tconvs, presumably because their TCRs have, on average, a higher affinity toward self-peptide. Analysis of CD5 expression in Treg precursors and thymic Tregs revealed that, in the absence of TCF7, the TCR-committed late Treg precursor and, especially, the differentiated thymic Tregs showed a strong increase in the percentage of CD5^{low} cells. This suggests that the pool of *Tcf7*-deficient thymic Tregs includes Tregs with lower TCR affinity (Fig. 6A).

To elaborate on the idea that loss, or lower levels, of TCF7 reduces the TCR avidity required to be selected into the Treg lineage, we crossed the *Nr4a1*-GFP reporter mouse with the *Tcf7*-deficient mouse. In the *Nr4a1*-GFP mouse model, activation of the transcription factor *Nr4a1* (*Nur77*), and therefore GFP expression, is directly correlated with TCR signaling strength (10). Analysis of the *Nr4a1*-GFP geometric mean showed that TCR signaling strength changes during the different phases of Treg development. It is lowest in the early Treg precursor, highest in the late Treg precursor, and settles at a median level for the more mature thymic Tregs (Fig. 6B). Comparison of *Nr4a1*-GFP expression in cells

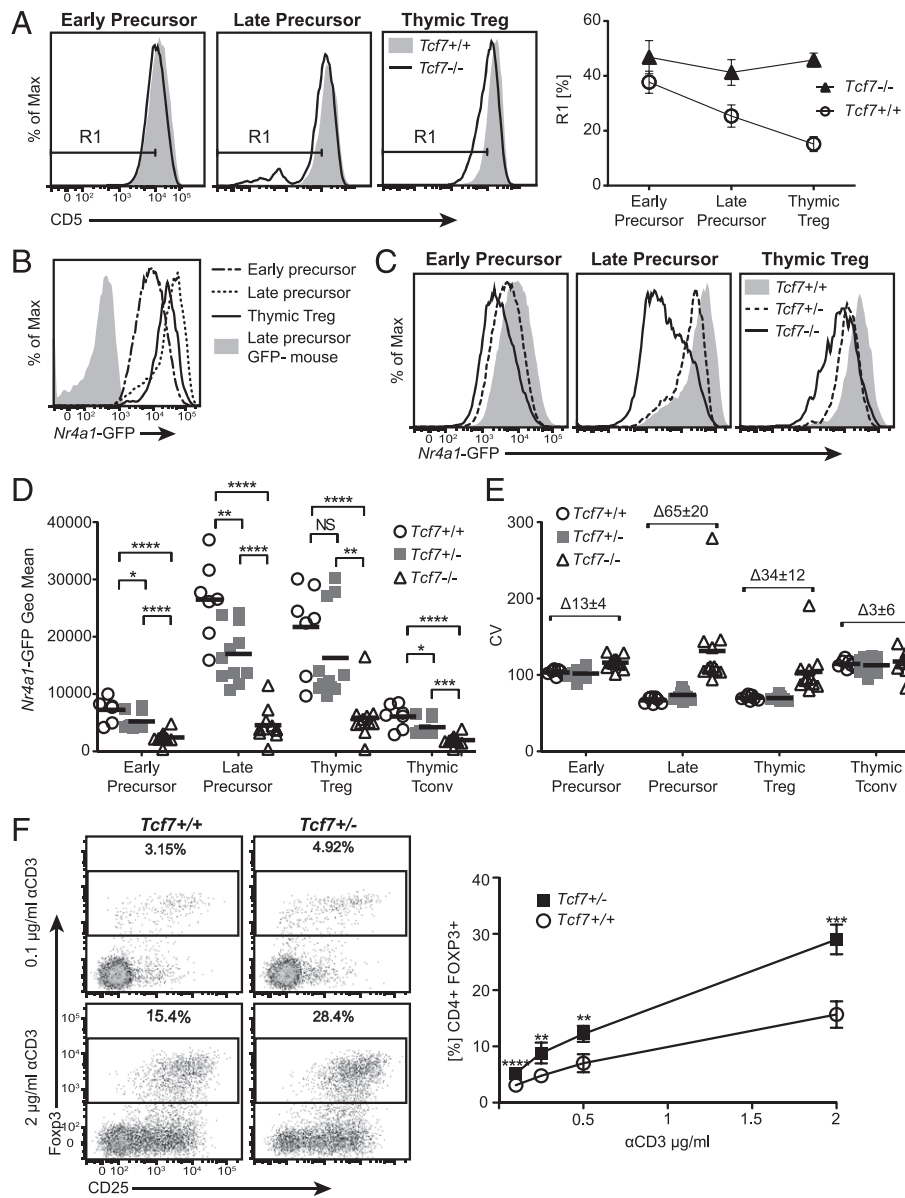
from *Tcf7⁺⁺*, *Tcf7^{+/−}*, and *Tcf7^{−−}* mice showed a population of late precursors and thymic Tregs with lower expression of *Nr4a1*-GFP in *Tcf7^{−−}* mice (Fig. 6C, 6D). This was due, in part, to a shift of cells with high GFP expression, but it primarily was due to the inclusion of cells with lower *Nr4a1*-GFP expression, indicating that the TCR signaling required to enter the Treg lineage was significantly lower in *Tcf7^{−−}* mice (Fig. 6C, 6D). This difference was already detectable in the TCR-committed late Treg precursor. In fact, the more TCF7 that was expressed, the more TCR signaling was required to enter the Treg lineage (Fig. 6C, 6D). To further study the phenomenon of a broadened TCR repertoire in committed precursors, thymic Tregs, and thymic Tconvs, we calculated the coefficient of variation as a standardized measure of dispersion or frequency distribution of the *Nr4a1*-GFP signal in the respective cell population of an individual thymus (Fig. 6E). Indeed, loss of TCF7 significantly broadened the TCR repertoire in the late precursor (65 ± 20 , $p = 0.005$) and thymic Tregs (34 ± 12 , $p = 0.01$) but not in thymic Tconvs (3 ± 6 , $p = 0.63$), thereby including cells with less TCR signaling (Fig. 6C, 6E). Interestingly, this difference was conserved and still detectable in peripheral spleen Tregs (Supplemental Fig. 3A).

To functionally address the TCR requirements to be selected into the Treg lineage, we modified our in vitro system to allow a range of TCR signal strengths. We changed the strong anti-CD3/CD28 bead-based stimulus to an anti-CD3 plate-bound system to allow titration of CD3 concentrations that mimic different TCR affinities. To this end, we added a fixed concentration of anti-CD28 and titrated the anti-CD3 Ab from 0.1 to 2 μ g/ml to compare the Treg-generation capacity. These experiments could not be done with Treg precursors from *Tcf7^{−−}* mice because these cells had problems surviving the in vitro culture conditions. Instead, we compared *Tcf7⁺⁺* and *Tcf7^{+/−}* early Treg precursors (Fig. 6F, Supplemental Fig. 3B). *Tcf7⁺⁺* Treg precursors produced significantly higher percentages of Tregs across all anti-CD3 concentrations tested. In fact, we calculated that precursors from *Tcf7⁺⁺* mice required approximately 3-fold more TCR stimulation to enter the Treg lineage, as determined by Ab concentration (Fig. 6F, Supplemental Fig. 3B). Therefore, normal levels of *Tcf7* in Treg precursors restrained the TCR-dependent differentiation into the Treg lineage. Together with the data obtained from the *Nr4a1*-GFP mice and CD5 experiments, these results indicate that tTregs generated under *Tcf7*-deficient conditions require less TCR stimulation and contain a larger proportion of cells with a lower TCR affinity.

Gain-of-function studies

To complement the TCF7 deficiency experiments with gain-of-function experiments, we tested Treg development following stimulation of the TCF7 pathway. Activation of TCF7 through β -catenin can be triggered by Wnt signaling (17, 24). We tested whether Wnt signaling could interfere with the development of Tregs from *Tcf7*-sufficient wild-type mice. To this end, the early Treg precursor was cultured in the anti-CD3/CD28 bead-based Treg-differentiation assay with two activators of the Wnt signaling pathway (Fig. 7A, 7B, Supplemental Fig. 3C, 3D). BIO and CHIR99021 are both inhibitors of the Wnt signaling negative regulator glycogen synthase kinase 3. Therefore, treatment with these inhibitors has an activating effect on Wnt signaling. Differentiation of the early Treg precursors in the presence of Wnt activators was reduced significantly compared with DMSO controls (Fig. 7A, 7B, Supplemental Fig. 3C, 3D).

Finally, we wanted to analyze how TCF7 activity is modulated during Treg differentiation, and we took a closer look at the relationship between FOXP3 and TCF7. This revealed that the



expression level of TCF7 is high in both Treg precursors (Fig. 7C). The TCF7 decrease coincided with the first expression of FOXP3. Therefore, we analyzed whether FOXP3 can influence TCF7 levels. To this end, we retrovirally overexpressed FOXP3 in Tconvs in vitro. Transduced T cells showed that expression of FOXP3 induces repression of TCF7 at the protein level (Fig. 7D), which could account for the reduced expression of TCF7 in differentiated tTregs.

In conclusion, the gain-of-function and loss-of-function data suggest that TCF7 interferes with the ability of Treg precursors to differentiate into mature tTregs, and FOXP3 can finally regulate the expression of regulator TCF7.

Discussion

Although generation of tTregs has been studied for years, this process is still not fully understood, and important regulators of this process are still being identified. Based on proteomics and gene expression data comparing Tregs and Tconvs, we identified TCF7 as a promising candidate. The proteomics data set with its 5225 identified proteins by itself is a valuable repository for further Treg research. Although proteomics has been used to study Tregs,

previous studies focused either on proteins identified by gel blotting (44) or selective differences in the expression of specific surface molecules (45) or protein kinases (46). One recent report used proteomics to study the FOXP3 complex with all of its interaction partners (47). We now provide a comprehensive quantitative and differential proteomics data set of murine Tregs and Tconvs. Together with our comparative analysis of proteome and gene expression data, we generated a data set that will assist in better understanding the uniqueness of Tregs.

Previous studies of the function of TCF7 in thymocyte development did not distinguish between Tconv and Treg subsets (15, 17, 19, 22, 24). We observed that TCF7 deficiency increased the fraction of Tregs among the CD4 SP and DP cell populations. This, by itself, does not prove that TCF7 is involved in processes that interfere with Treg selection, because the severe reduction in the total number of thymocytes could also influence the Tconv compartment. Therefore, we continued to work with *Tcf7*-heterozygous mice. We demonstrated that Treg precursors from heterozygous mice expressed about half of the *Tcf7* message, and this decreased TCF7 level led to the enhanced Treg-differentiation capacity of Treg precursors. We carefully

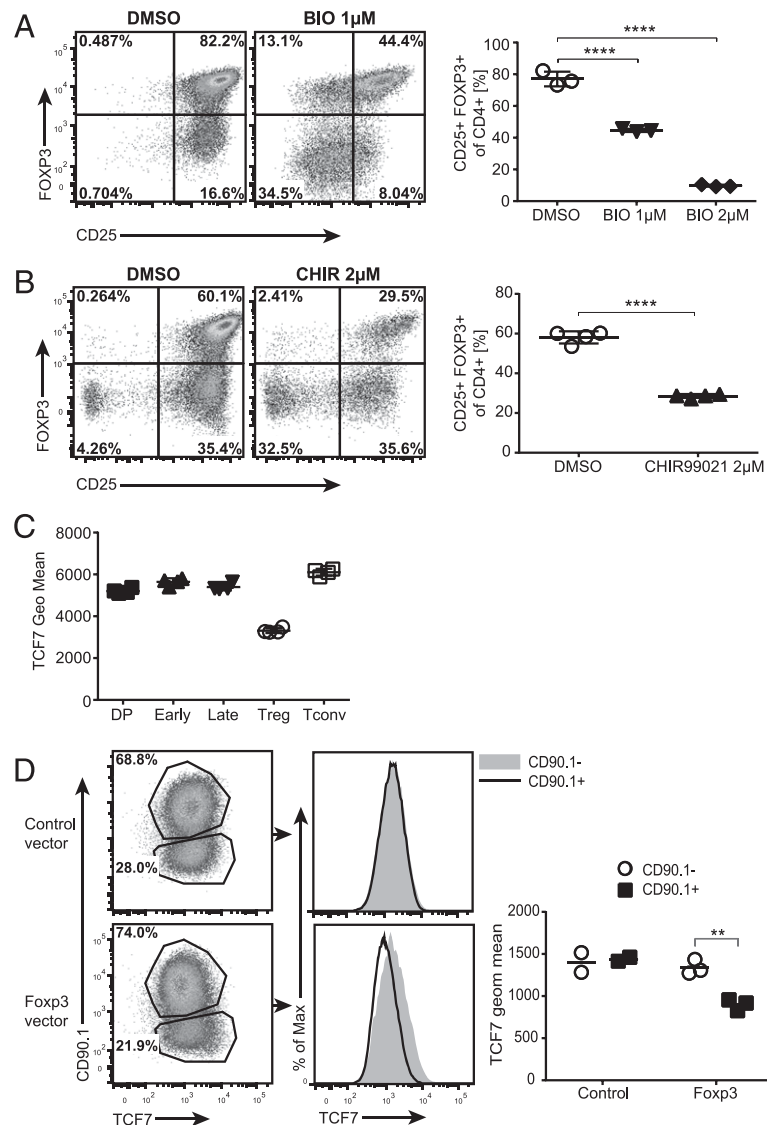


FIGURE 7. Gain of function. Treg generation after culture in the presence of Wnt activators BIO at 1 or 2 μ M (**A**) and CHIR99021 at 2 μ M (**B**) ($n = 3–4$). Control cells were cultured with DMSO. The early Treg precursor was FACS purified from *Foxp3*-GFP⁺ mice and cultured for 3 d with IL-2, IL-15, and anti-CD3/28. (**C**) TCF7 expression in different thymic populations from wild-type B6 mice ($n = 4$). (**D**) Retroviral overexpression of control vector (CD90.1⁺) or FOXP3 vector (CD90.1⁺ and FOXP3⁺) in T cells 3 d after transduction. CD90.1 and TCF7 expression in transduced T cells (*left panels*). TCF7 expression in CD90.1⁻ and CD90.1⁺ T cells (*middle panels*). Quantification of TCF7 expression in CD90.1⁻ and CD90.1⁺ cells. Representative data from two independent experiments are shown. Symbols represent individual mice, and numbers indicate the percentage of cells within the defined region. The horizontal lines indicate the mean value for each group. ** $p < 0.01$, **** $p < 0.0001$, unpaired t test.

FACS purified TCR-rearranged (i.e., postpositive selection) Treg precursors and studied them in vitro, in the absence of other thymic influences, to determine their ability to differentiate into Tregs. We purposely used an APC-free Treg-differentiation system to control for the number of signals received by the Treg precursors. An APC-free thymic Treg precursor-differentiation assay was introduced previously (14). In this study, the investigators demonstrated that, on day 3, ~10% of cells had differentiated into FOXP3⁺ Tregs (14). We refined this assay by introducing an anti-CD3/CD28 bead-based stimulus and different cytokine conditions and were able to improve the efficiency of Treg lineage commitment to up to 80% after 3 d. Importantly, thymic Tconvs (CD4PS CD69⁻) had generally lost the ability to differentiate into Tregs under the same conditions, indicating that Treg commitment is restricted to a narrow developmental window. These data showed that three signals were sufficient for Treg differentiation: TCR, costimulation, and common γ -chain signaling. TCF7 has to interfere with one of these three signals, because the endogenous TCF7 levels in wild-type Treg precursors restrict Treg development under these conditions. Indeed, it was shown that β -catenin and TCF7 signaling were active downstream of TCR signaling (24). When we titrated the TCR stimulus by using different concentrations of anti-CD3, we observed that wild-type levels of TCF7 in Treg precursors limited Treg output over a broad range of stimuli. We

calculated that heterozygote precursors with reduced TCF7 levels needed about three times less TCR stimulus compared with Treg precursors from *Tcf7* wild-type mice. This indicated that TCF7 increases the requirements of the TCR stimulus for a Treg precursor to differentiate into the Treg lineage and, thereby, helps to move the critical window of Treg commitment to higher-affinity TCR interactions. This idea was supported by our findings in the *Nr4a1*-GFP mouse. Previous studies described the *Nr4a1*-GFP reporter mouse as a tool to investigate the TCR avidities in developing T cells and Tregs, because the GFP expression correlates with TCR signaling strength (10, 48). In *Tcf7*-deficient precursors and thymic Tregs, we detected cells with lower expression of *Nr4a1* indicating less TCR affinity, which supports the concept that TCF7 fosters the selection of clones with higher TCR affinities. This observation was also supported by our finding that tTregs from *Tcf7*-deficient mice harbor many more CD5^{low} Tregs. In contrast, although thymic Tconvs from *Nr4a1*-deficient mice also had lower expression of *Nr4a1*, there was no difference in the breadth of the TCR affinities compared with *Tcf7*-sufficient mice. Of note, this analysis also showed that the distribution of affinities in late Treg precursors, as well as thymic Tregs, was significantly lower than that in thymic Tconvs, which supports the concept that Tregs are normally selected in a more narrow TCR affinity range compared with Tconvs.

Other factors have been implicated with such a modulatory effect on the TCR signal. Themis was proposed to control the signaling threshold for positive and negative selection, although Treg development was not analyzed in that study (49). Another recent report suggested that TNFR family members, such as GITR and OX40, could couple TCR signal strength to tTreg differentiation (48). Unlike these TNFR family members that support Treg differentiation by lowering the required TCR threshold, TCF7 could act antagonistically to restrict generation, exclude low TCR affinities, and, thereby, help to shape the Treg TCR repertoire toward higher-affinity clones. Interestingly, a recent study demonstrated that Tregs from *Tcf7*-deficient mice are perfectly functional and, if anything, were even more potent in suppression assays (50).

It was observed recently that activation of β -catenin results in significantly fewer Tregs in the thymus (51). Using CD4-specific expression of constitutively active β -catenin and BM chimeras, it was shown that this effect was T cell intrinsic. We took this analysis one step further by demonstrating that Treg precursors are sensitive to TCF7/ β -catenin signaling. In the thymus, TCF7 signaling can be triggered through different pathways. For example, in early T cell precursors, Notch signaling was also shown to induce TCF7 (19, 20). It is unclear which signaling events are more critical for TCF7 induction and, thereby, interference with Treg differentiation. Intriguingly, once FOXP3 is expressed it can facilitate a reduced expression level of TCF7 and, thus, may foster a survival advantage in committed Tregs.

The molecular basis of how a biased TCR repertoire is established in developing tTregs is still not fully understood. Our results suggest that TCF7 is part of this program and helps to restrict and shape the TCR repertoire toward higher-affinity clones that access the Treg lineage. By increasing the TCR signaling strength hurdle, TCF7 may contribute to the enrichment of self-reactive TCRs within the Treg pool.

Acknowledgments

We thank all contributors to this study: H. Clevers for providing the TCF7^{-/-} mouse, A. Rudensky (Memorial Sloan-Kettering Cancer Center, New York, NY) for providing Foxp3 YFP/Cre and Foxp3 DTR/GFP mice, B. Kyewski (German Cancer Research Center) for reading the manuscript and valuable discussions, F. Brunk (German Cancer Research Center) for help with the Wnt signaling assay, K. Lobbes and E. Lederer for excellent technical support, the European Molecular Biology Laboratory Proteomics Core Facility for expert assistance, the Central Animal Laboratory, and the Flow Cytometry core facilities (German Cancer Research Center).

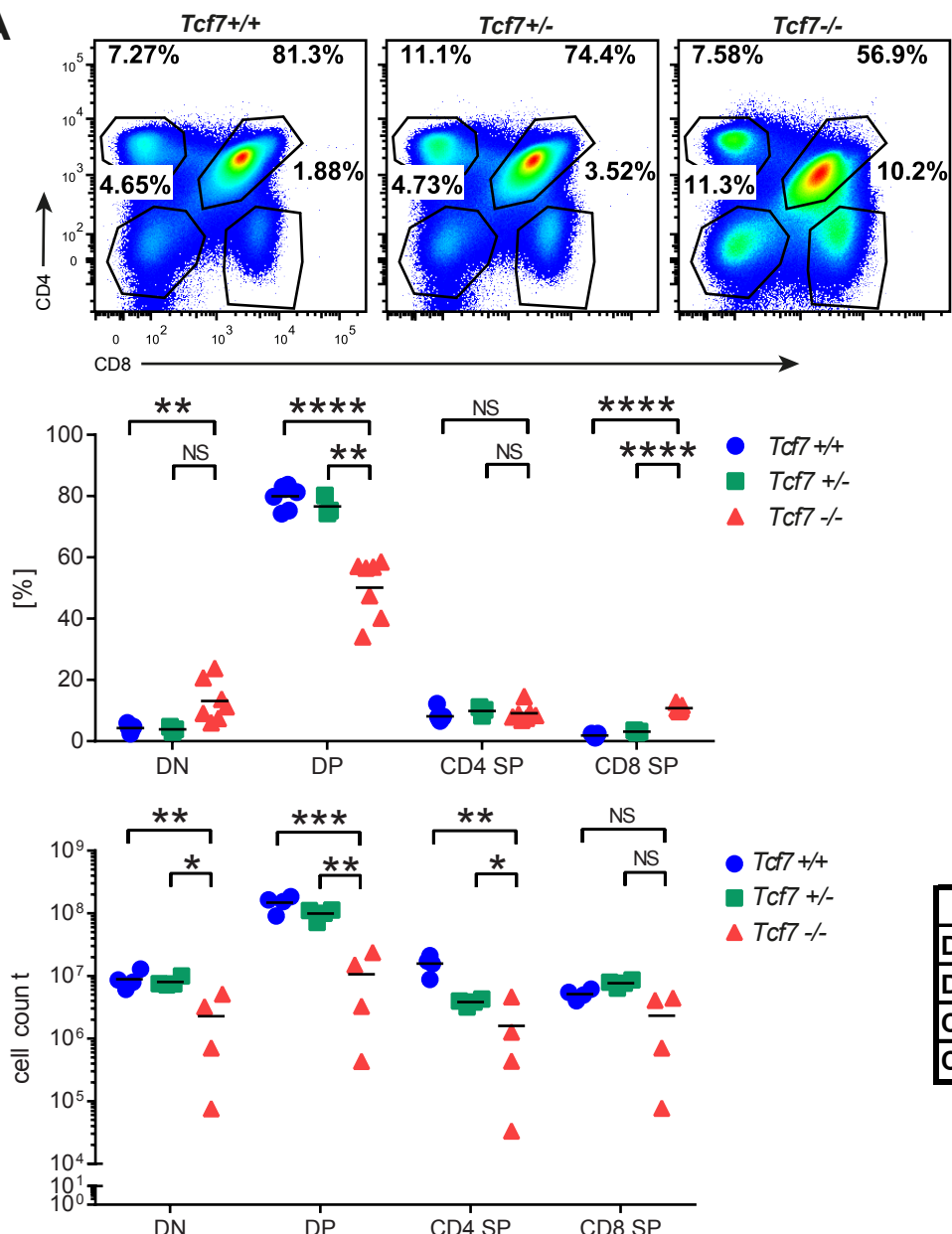
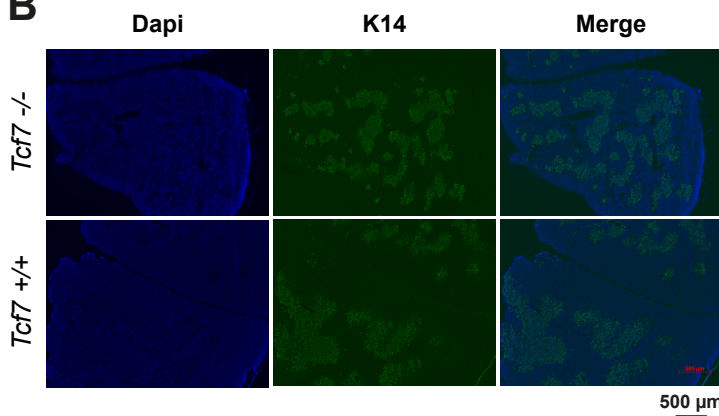
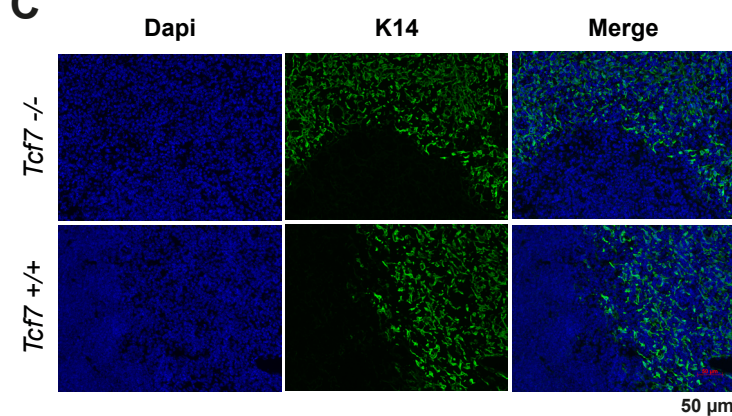
Disclosures

The authors have no financial conflicts of interest.

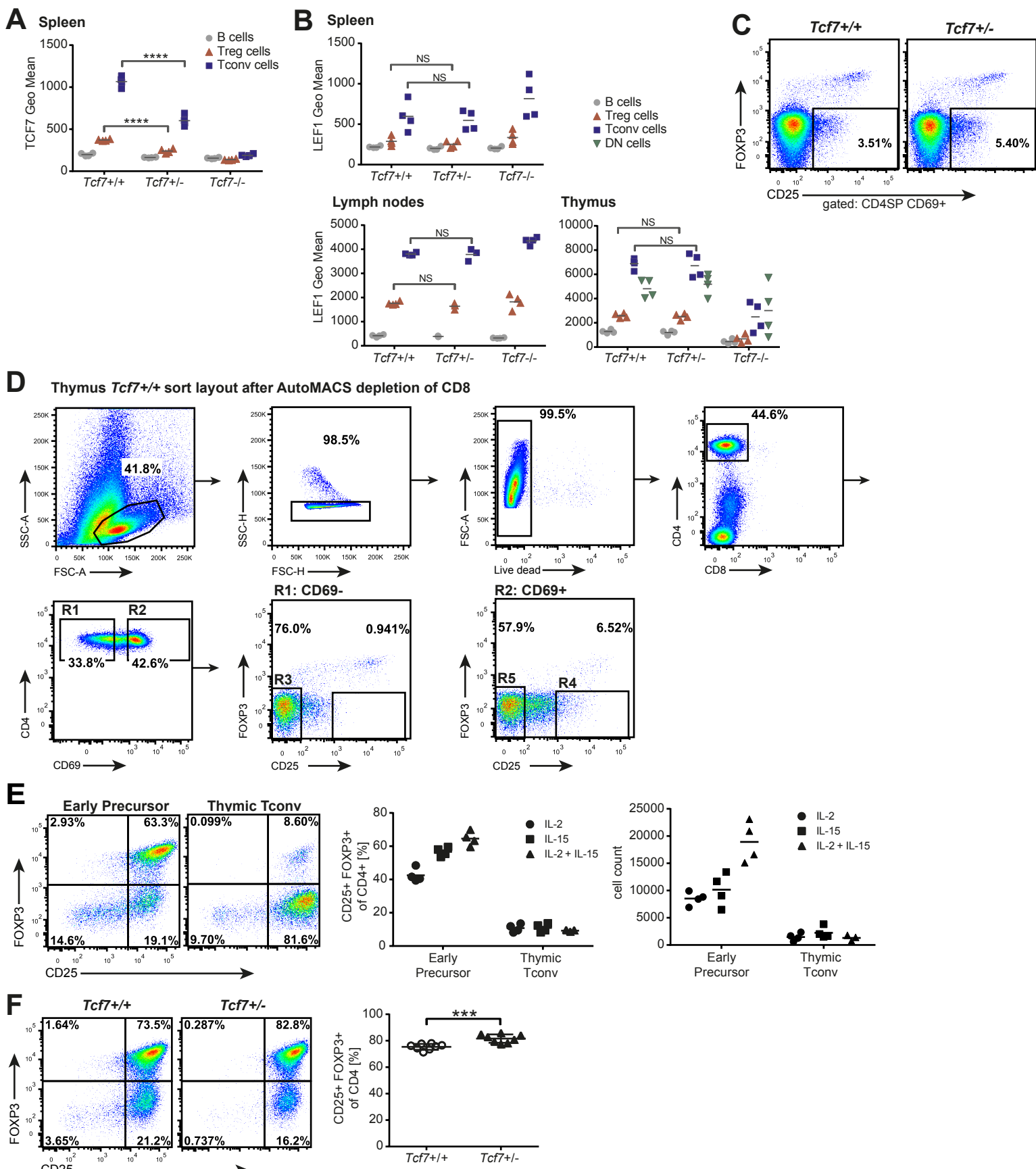
References

- Fontenot, J. D., M. A. Gavin, and A. Y. Rudensky. 2003. Foxp3 programs the development and function of CD4+CD25+ regulatory T cells. *Nat. Immunol.* 4: 330–336.
- Hori, S., T. Nomura, and S. Sakaguchi. 2003. Control of regulatory T cell development by the transcription factor Foxp3. *Science* 299: 1057–1061.
- Khattri, R., T. Cox, S. A. Yasayko, and F. Ramsdell. 2003. An essential role for Scurfin in CD4+CD25+ T regulatory cells. *Nat. Immunol.* 4: 337–342.
- Sakaguchi, S. 2004. Naturally arising CD4+ regulatory T cells for immunologic self-tolerance and negative control of immune responses. *Annu. Rev. Immunol.* 22: 531–562.
- Hsieh, C. S., H. M. Lee, and C. W. Lio. 2012. Selection of regulatory T cells in the thymus. *Nat. Rev. Immunol.* 12: 157–167.
- Rothenberg, E. V., and T. Taghon. 2005. Molecular genetics of T cell development. *Annu. Rev. Immunol.* 23: 601–649.
- Hsieh, C. S., Y. Liang, A. J. Tyznik, S. G. Self, D. Liggitt, and A. Y. Rudensky. 2004. Recognition of the peripheral self by naturally arising CD25+CD4+ T cell receptors. *Immunity* 21: 267–277.
- Pacholczyk, R., H. Ignatowicz, P. Kraj, and L. Ignatowicz. 2006. Origin and T cell receptor diversity of Foxp3+CD4+CD25+ T cells. *Immunity* 25: 249–259.
- Wong, J., R. Obst, M. Correia-Neves, G. Losyev, D. Mathis, and C. Benoist. 2007. Adaptation of TCR repertoires to self-peptides in regulatory and non-regulatory CD4+ T cells. *J. Immunol.* 178: 7032–7041.
- Moran, A. E., K. L. Holzapfel, Y. Xing, N. R. Cunningham, J. S. Maltzman, J. Punt, and K. A. Hogquist. 2011. T cell receptor signal strength in Treg and iNKT cell development demonstrated by a novel fluorescent reporter mouse. *J. Exp. Med.* 208: 1279–1289.
- Bautista, J. L., C. W. Lio, S. K. Lathrop, K. Forbush, Y. Liang, J. Luo, A. Y. Rudensky, and C. S. Hsieh. 2009. Intralonal competition limits the fate determination of regulatory T cells in the thymus. *Nat. Immunol.* 10: 610–617.
- Salomon, B., D. J. Lenschow, L. Rhee, N. Ashourian, B. Singh, A. Sharpe, and J. A. Bluestone. 2000. B7/CD28 costimulation is essential for the homeostasis of the CD4+CD25+ immunoregulatory T cells that control autoimmune diabetes. *Immunity* 12: 431–440.
- Lio, C. W., and C. S. Hsieh. 2008. A two-step process for thymic regulatory T cell development. *Immunity* 28: 100–111.
- Wirnsberger, G., F. Mair, and L. Klein. 2009. Regulatory T cell differentiation of thymocytes does not require a dedicated antigen-presenting cell but is under T cell-intrinsic developmental control. *Proc. Natl. Acad. Sci. USA* 106: 10278–10283.
- Verbeek, S., D. Izon, F. Hofhuis, E. Robanus-Maandag, H. te Riele, M. van de Wetering, M. Oosterwegel, A. Wilson, H. R. MacDonald, and H. Clevers. 1995. An HMG-box-containing T-cell factor required for thymocyte differentiation. *Nature* 374: 70–74.
- Schilham, M. W., A. Wilson, P. Moerer, B. J. Benaiissa-Trouw, A. Cumano, and H. C. Clevers. 1998. Critical involvement of Tcf-1 in expansion of thymocytes. *J. Immunol.* 161: 3984–3991.
- Staal, F. J., T. C. Luis, and M. M. Tiemessen. 2008. WNT signalling in the immune system: WNT is spreading its wings. *Nat. Rev. Immunol.* 8: 581–593.
- Barra, M. M., D. M. Richards, A. C. Hofer, M. Delacher, and M. Feuerer. 2015. Premature expression of foxp3 in double-negative thymocytes. *PLoS One* 10: e0127038.
- Weber, B. N., A. W. Chi, A. Chavez, Y. Yashiro-Ohtani, Q. Yang, O. Shestova, and A. Bhandoola. 2011. A critical role for TCF-1 in T-lineage specification and differentiation. *Nature* 476: 63–68.
- Germar, K., M. Dose, T. Konstantinou, J. Zhang, H. Wang, C. Lobry, K. L. Arnett, S. C. Blacklow, I. Aifantis, J. C. Aster, and F. Gounari. 2011. T-cell factor 1 is a gatekeeper for T-cell specification in response to Notch signaling. *Proc. Natl. Acad. Sci. USA* 108: 20060–20065.
- Yu, S., X. Zhou, F. C. Steinke, C. Liu, S. C. Chen, O. Zagorodna, X. Jing, Y. Yokota, D. K. Meyerholz, C. G. Mullighan, et al. 2012. The TCF-1 and LEF-1 transcription factors have cooperative and opposing roles in T cell development and malignancy. [Published erratum appears in 2014 *Immunity* 40: 166.] *Immunity* 37: 813–826.
- Steinke, F. C., S. Yu, X. Zhou, B. He, W. Yang, B. Zhou, H. Kawamoto, J. Zhu, K. Tan, and H. H. Xue. 2014. TCF-1 and LEF-1 act upstream of Th-POK to promote the CD4(+) T cell fate and interact with Runx3 to silence Cd4 in CD8(+) T cells. *Nat. Immunol.* 15: 646–656.
- Ioannidis, V., F. Beermann, H. Clevers, and W. Held. 2001. The beta-catenin-TCF-1 pathway ensures CD4(+)CD8(+) thymocyte survival. *Nat. Immunol.* 2: 691–697.
- Kovalovsky, D., Y. Yu, M. Dose, A. Emmanouilidou, T. Konstantinou, K. Germar, K. Aghajani, Z. Guo, M. Mandal, and F. Gounari. 2009. Beta-catenin/Tcf determines the outcome of thymic selection in response to alpha-beta TCR signaling. *J. Immunol.* 183: 3873–3884.
- Feuerer, M., J. A. Hill, K. Kretschmer, H. von Boehmer, D. Mathis, and C. Benoist. 2010. Genomic definition of multiple ex vivo regulatory T cell subphenotypes. *Proc. Natl. Acad. Sci. USA* 107: 5919–5924.
- Feuerer, M., J. A. Hill, D. Mathis, and C. Benoist. 2009. Foxp3+ regulatory T cells: differentiation, specification, subphenotypes. *Nat. Immunol.* 10: 689–695.
- Heng, T. S., M. W. Painter, Immunological Genome Project Consortium, and K. Elpek, V. Lukacs-Kornek, N., S. J. Mauermann, D. Turley, F. S. Koller, A. J. Kim, Wagers, et al. 2008. The Immunological Genome Project: networks of gene expression in immune cells. *Nat. Immunol.* 9: 1091–1094.
- Hill, J. A., M. Feuerer, K. Tash, S. Haxhinasto, J. Perez, R. Melamed, D. Mathis, and C. Benoist. 2007. Foxp3 transcription-factor-dependent and -independent regulation of the regulatory T cell transcriptional signature. *Immunity* 27: 786–800.
- Rubtsov, Y. P., J. P. Rasmussen, E. Y. Chi, J. Fontenot, L. Castelli, X. Ye, P. Treuting, L. Siewe, A. Roers, W. R. Henderson, Jr., et al. 2008. Regulatory T cell-derived interleukin-10 limits inflammation at environmental interfaces. *Immunity* 28: 546–558.
- Kim, J. M., J. P. Rasmussen, and A. Y. Rudensky. 2007. Regulatory T cells prevent catastrophic autoimmunity throughout the lifespan of mice. *Nat. Immunol.* 8: 191–197.
- Boersema, P. J., R. Rajmakers, S. Lemeer, S. Mohammed, and A. J. Heck. 2009. Multiplex peptide stable isotope dimethyl labeling for quantitative proteomics. *Nat. Protoc.* 4: 484–494.
- Cox, J., and M. Mann. 2008. MaxQuant enables high peptide identification rates, individualized p.p.b.-range mass accuracies and proteome-wide protein quantification. *Nat. Biotechnol.* 26: 1367–1372.
- Gentleman, R. C., V. J. Carey, D. M. Bates, B. Bolstad, M. Dettling, S. Dudoit, B. Ellis, L. Gautier, Y. Ge, J. Gentry, et al. 2004. Bioconductor: open software development for computational biology and bioinformatics. *Genome Biol.* 5: R80.
- Smyth, G. K. 2004. Linear models and empirical bayes methods for assessing differential expression in microarray experiments. *Stat. Appl. Genet. Mol. Biol.* 3: Article3.

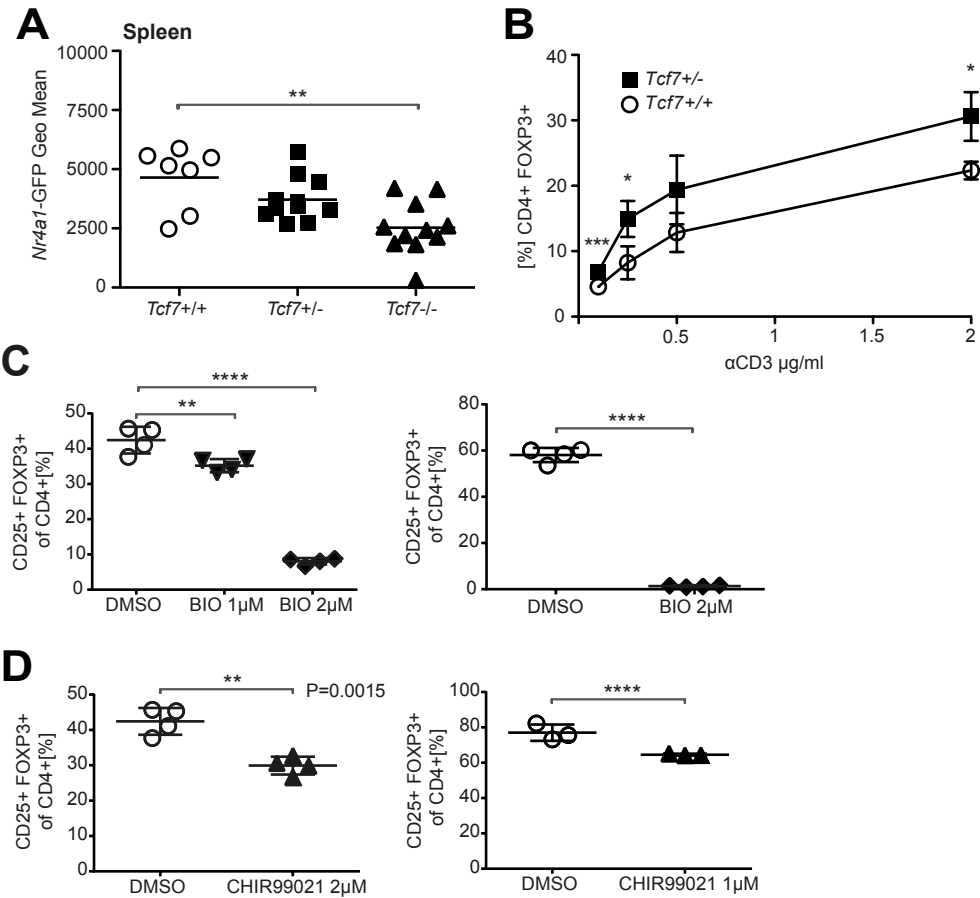
35. Jensen, L. J., M. Kuhn, M. Stark, S. Chaffron, C. Creevey, J. Muller, T. Doerks, P. Julien, A. Roth, M. Simonovic, et al. 2009. STRING 8—a global view on proteins and their functional interactions in 630 organisms. *Nucleic Acids Res.* 37: D412–D416.
36. Shannon, P., A. Markiel, O. Ozier, N. S. Baliga, J. T. Wang, D. Ramage, N. Amin, B. Schwikowski, and T. Ideker. 2003. Cytoscape: a software environment for integrated models of biomolecular interaction networks. *Genome Res.* 13: 2498–2504.
37. Vizcaíno, J. A., R. G. Côté, A. Csordas, J. A. Dianes, A. Fabregat, J. M. Foster, J. Griss, E. Alpi, M. Birim, J. Contell, et al. 2013. The PRoteomics IDEntifications (PRIDE) database and associated tools: status in 2013. *Nucleic Acids Res.* 41: D1063–D1069.
38. Beyer, M., Y. Thabet, R. U. Müller, T. Sadlon, S. Classen, K. Lahli, S. Basu, X. Zhou, S. L. Bailey-Bucktrout, W. Krebs, et al. 2011. Repression of the genome organizer SATB1 in regulatory T cells is required for suppressive function and inhibition of effector differentiation. *Nat. Immunol.* 12: 898–907.
39. Gavin, M. A., J. P. Rasmussen, J. D. Fontenot, V. Vasta, V. C. Manganiello, J. A. Beavo, and A. Y. Rudensky. 2007. Foxp3-dependent programme of regulatory T-cell differentiation. *Nature* 445: 771–775.
40. Gomez-Rodriguez, J., E. A. Wohlfert, R. Handon, F. Meylan, J. Z. Wu, S. M. Anderson, M. R. Kirby, Y. Belkaid, and P. L. Schwartzberg. 2014. Itk-mediated integration of T cell receptor and cytokine signaling regulates the balance between Th17 and regulatory T cells. *J. Exp. Med.* 211: 529–543.
41. Mingueneau, M., T. Kreslavsky, D. Gray, T. Heng, R. Cruse, J. Ericson, S. Bendall, M. H. Spitzer, G. P. Nolan, K. Kobayashi, et al. 2013. The transcriptional landscape of $\alpha\beta$ T cell differentiation. *Nat. Immunol.* 14: 619–632.
42. Fontenot, J. D., J. P. Rasmussen, L. M. Williams, J. L. Dooley, A. G. Farr, and A. Y. Rudensky. 2005. Regulatory T cell lineage specification by the forkhead transcription factor foxp3. *Immunity* 22: 329–341.
43. Azzam, H. S., A. Grinberg, K. Lui, H. Shen, E. W. Shores, and P. E. Love. 1998. CD5 expression is developmentally regulated by T cell receptor (TCR) signals and TCR avidity. *J. Exp. Med.* 188: 2301–2311.
44. Kubach, J., P. Lutter, T. Bopp, S. Stoll, C. Becker, E. Huter, C. Richter, P. Weingarten, T. Warger, J. Knop, et al. 2007. Human CD4+CD25+ regulatory T cells: proteome analysis identifies galectin-10 as a novel marker essential for their anergy and suppressive function. *Blood* 110: 1550–1558.
45. Solstad, T., S. J. Bains, J. Landskron, E. M. Aandahl, B. Thiede, K. Taskén, and K. M. Torgersen. 2011. CD147 (Basigin/Emmprin) identifies FoxP3+CD45RO +CTLA4+-activated human regulatory T cells. *Blood* 118: 5141–5151.
46. König, S., M. Probst-Kepper, T. Reinal, A. Jeron, J. Huehn, B. Schraven, and L. Jänsch. 2012. First insight into the kinome of human regulatory T cells. *PLoS One* 7: e40896.
47. Rudra, D., P. deRoos, A. Chaudhry, R. E. Niec, A. Arvey, R. M. Samstein, C. Leslie, S. A. Shaffer, D. R. Goodlett, and A. Y. Rudensky. 2012. Transcription factor Foxp3 and its protein partners form a complex regulatory network. *Nat. Immunol.* 13: 1010–1019.
48. Mahmud, S. A., L. S. Manlove, H. M. Schmitz, Y. Xing, Y. Wang, D. L. Owen, J. M. Schenkel, J. S. Boomer, J. M. Green, H. Yagita, et al. 2014. Costimulation via the tumor-necrosis factor receptor superfamily couples TCR signal strength to the thymic differentiation of regulatory T cells. *Nat. Immunol.* 15: 473–481.
49. Fu, G., J. Casas, S. Rigaud, V. Rybakin, F. Lambolez, J. Brzostek, J. A. Hoerter, W. Paster, O. Acuto, H. Cheroutre, et al. 2013. Themis sets the signal threshold for positive and negative selection in T-cell development. *Nature* 504: 441–445.
50. van Loosdregt, J., V. Fleskens, M. M. Tiemessen, M. Mokry, R. van Boxtel, J. Meerdink, C. E. Pals, D. Kurek, M. R. Baert, E. M. Delemarre, et al. 2013. Canonical Wnt signaling negatively modulates regulatory T cell function. *Immunity* 39: 298–310.
51. Keerthivasan, S., K. Aghajani, M. Dose, L. Molinero, M. W. Khan, V. Venkateswaran, C. Weber, A. O. Emmanuel, T. Sun, D. J. Bentrem, et al. 2014. β -Catenin promotes colitis and colon cancer through imprinting of proinflammatory properties in T cells. *Sci. Transl. Med.* 6: 225ra28.

A**B****C**

Supplemental Figure 1. Analysis of thymic populations by flow cytometry and microscopy. (A) Upper panel: representative dot plots of thymic CD4 and CD8 populations in Tcf7^{+/+}, Tcf7^{+/-} and Tcf7^{-/-} mice. Middle panel: quantified percentages of DN, DP, CD4SP and CD8SP populations pre-gated on CD11b-CD11c-CD19- thymocytes. Lower panel: quantified cell counts of DN, DP, CD4SP and CD8SP populations from total thymus. Embedded table shows fold change of the average cell count between Tcf7^{+/+} and Tcf7^{-/-} from DN, DP, CD4SP and CD8SP populations. Symbols represent individual mice and the horizontal lines indicate the mean value for each group. All cell counts were performed using counting beads. (B and C) Immunofluorescence imaging of K14⁺ medullary epithelial cells from Tcf7^{+/+} and Tcf7^{-/-} thymus. Representative data from 2 to 3 individual thymus is shown (B) 2.5-fold magnification and 500 µm scale bar, (C) 20-fold magnification and 50 µm scale bar. NS, P > 0.05, * P < 0.05, ** P < 0.01, *** P < 0.001, **** P < 0.0001 (unpaired t-test or ordinary one-way ANOVA).



Supplemental Figure 2. Dosage effect of TCF7. (A-B) Analysis of TCF7 (A) and LEF1 (B) expression in Treg, Tconv, DN and B cells from Tcf7^{+/+}, Tcf7^{+/-} and Tcf7^{-/-} mice (n=4). (C) Analysis of late Treg precursors from Tcf7^{+/+} and Tcf7^{+/-} mice. Representative plots correspond to Fig. 5G. (D) FACS scheme for Tcf7^{+/+} Foxp3-YFP⁺ thymi after MACS depletion of CD8⁺ cells. R1: CD4SP CD69⁻; R2: CD4SP CD69⁺; R3: CD4SP CD69-CD25-Foxp3⁻ (thymic Tconv); R4: CD4SP CD69⁺CD25⁺ Foxp3⁻ (late Treg precursor); R5: CD4SP CD69⁺CD25-Foxp3⁻ (early Treg precursor). (E) FACS-purified early Treg precursor was cultured for 3 days under different conditions (as depicted) with anti-CD3/CD28 beads. Thymic Tconv cells were used as a control (n=3-4). Analysis and cell counts were performed by flow cytometry. (F) Incubation of early precursors from Tcf7^{+/+} or Tcf7^{+/-} Foxp3-YFP⁺ mice with IL-2, IL-15 and anti-CD3/CD28 beads (n=8). Symbols represent individual samples and the horizontal lines indicate the mean value for each group. NS, P > 0.05, *** P < 0.001, **** P < 0.0001 (unpaired t test).



Supplemental Figure 3. TCR stimulus and activation of Wnt signaling. (A) Quantification of Nr4a1-GFP expression in Treg cells from the spleens of *Tcf7*^{+/+}, *Tcf7*^{+/-} and *Tcf7*^{-/-} Nr4a1-GFP mice (n=7-12). (B) Early Treg precursors were FACS-purified from *Tcf7*^{+/+} or *Tcf7*^{+/-} Foxp3-YFP⁺ mice. The cells were cultured for 3 days in vitro on plates coated with 0.1, 0.25, 0.5 or 2 µg/ml of anti-CD3. IL-2, IL-15 anti-CD28 were added to the culture (n=3). Quantified percentages of CD4+ Foxp3⁺ cells generated from *Tcf7*^{+/+} and *Tcf7*^{+/-} precursors is shown, independent repeat experiment of Fig. 6F. (C-D) Early Treg precursors were FACS-purified from Foxp3-GFP⁺ mice. The cells were cultured for 3 days in vitro with IL-2, IL-15 and anti-CD3/CD28 (n = 3-4) in the presence of Wnt activators or DMSO. Percentages of CD4+ CD25+Foxp3⁺ Treg cells were assessed by flow cytometry. (C) Quantified results of two individual experiments with the Wnt activator BIO. Left panel: BIO at 1 and 2 µM. Right panel: BIO at 2 µM. (D) Quantified results of two individual experiments with the Wnt activator CHIR99021. Left panel: CHIR99021 at 2 µM. Right panel: CHIR99021 at 1 µM. Symbols represent individual samples and the horizontal lines indicate the mean value for each group. NS, P > 0.05, * P < 0.05, ** P < 0.01, *** P < 0.001, **** P < 0.0001 (unpaired t-test).